Advances in Water Resources 97 (2016) 205–218

Contents lists available at ScienceDirect

Advances in Water Resources

journal homepage: www.elsevier.com/locate/advwatres

Improving radar rainfall estimation by merging point rainfall measurements within a model combination framework

Mohammad Mahadi Hasan[a], Ashish Sharma[a,*], Gregoire Mariethoz[a,b], Fiona Johnson[a], Alan Seed[a,c]

[a] School of Civil and Environmental Engineering, University of New South Wales, Sydney, NSW 2052, Australia
[b] University of Lausanne, Institute of Earth Surface Dynamics, Switzerland
[c] Research and Development, Bureau of Meteorology, Australia

ARTICLE INFO

Article history:
Received 20 April 2016
Revised 13 September 2016
Accepted 20 September 2016
Available online 22 September 2016

Keywords:
Radar reflectivity
Nonparametric radar rainfall
Spatial interpolation
Merging radar and gauge rainfall
Weighted combination
Spatial and temporal

ABSTRACT

While the value of correcting raw radar rainfall estimates using simultaneous ground rainfall observations is well known, approaches that use the complete record of both gauge and radar measurements to provide improved rainfall estimates are much less common. We present here two new approaches for estimating radar rainfall that are designed to address known limitations in radar rainfall products by using a relatively long history of radar reflectivity and ground rainfall observations. The first of these two approaches is a radar rainfall estimation algorithm that is nonparametric by construction. Compared to the traditional gauge adjusted parametric relationship between reflectivity (Z) and ground rainfall (R), the suggested new approach is based on a nonparametric radar rainfall estimation method (NPR) derived using the conditional probability distribution of reflectivity and gauge rainfall. The NPR method is applied to the densely gauged Sydney Terrey Hills radar network, where it reduces the RMSE in rainfall estimates by 10%, with improvements observed at 90% of the gauges. The second of the two approaches is a method to merge radar and spatially interpolated gauge measurements. The two sources of information are combined using a dynamic combinatorial algorithm with weights that vary in both space and time. The weight for any specific period is calculated based on the error covariance matrix that is formulated from the radar and spatially interpolated rainfall errors of similar reflectivity periods in a cross-validation setting. The combination method reduces the RMSE by about 20% compared to the traditional Z-R relationship method, and improves estimates compared to spatially interpolated point measurements in sparsely gauged areas.

1. Introduction

Accurate rainfall estimates are of great importance in hydrology. Rain gauges and weather radars are the two most widely used sensors for rainfall measurement (Severino and Alpuim, 2005; Habib et al., 2001; Berne et al., 2005). Rain gauges are a simple and cheap technology providing relatively accurate measurements at a point location. In contrast, weather radars provide estimations of rainfall over large geographic areas with the benefit of repeated measurements at high frequency (García-Pintado et al., 2009). Radar measures the strength of electromagnetic waves backscattered by the atmosphere, termed as 'Reflectivity' . Conventionally, a power law relationship often referred to as the Z-R relationship ($Z=AR^b$) is used to relate the radar reflectivities (Z) to ground rainfall rates (R) (Krajewski and Smith, 2002; Mapiam et al., 2009). In most situations, the process of radar rainfall estimation involves (1) the measurement of reflectivity, (2) the removal of errors caused during its measurement, (3) the conversion of estimated reflectivity into rainfall, and 4) an adjustment depending on gauge rainfall measurements (Chumchean et al., 2006a). Uncertainties are associated with each of these steps. In practice, when considering long duration rainfall periods and/or multiple storm types, steps (1) and (2) can be affected by phenomena such as ground clutter, beam blockage, anomalous propagation, hail, bright band, attenuation, range-dependent bias, range degradation, vertical profile of reflectivity, temporal and spatial sampling errors (Chumchean et al., 2006; Villarini and Krajewski, 2010). There are also errors introduced by rainfall variability and precipitation drift as well as the uncertainties of relating point rainfall measurements to radar measurements across a gridded domain. Our aim is to address the uncertainties in converting the radar reflectivity to rainfall rates that have

* Corresponding author. Fax: +61 2 9385 6139.
E-mail address: a.sharma@unsw.edu.au (A. Sharma).

http://dx.doi.org/10.1016/j.advwatres.2016.09.011

hampered the widespread use of radars in hydrology (Villarini and Krajewski, 2010).

It has been shown that improved rainfall estimates can be achieved through a combination of radar and gauge measurements by exploiting their strengths and correcting for their shortcomings (Schiemann et al., 2011; Burlando et al., 1996; Krajewski, 1987). This paper proposes two innovative methods for improving radar rainfall estimation by combining gauge and radar measurements. The idea of merging radar and gauge measurement is not new and a number of different methods have been developed. Previous studies were mostly concerned about the application of gauge data for correcting systematic errors in radar rainfall estimates. The most common application is Mean Field Bias (MFB) correction of radar rainfall estimates (Chumchean et al., 2006a; Seo, 1998). It considers a multiplicative adjustment factor estimated as the ratio of the accumulated radar rainfall and the accumulated gauge rainfall (Kitzmiller et al., 2013). Though MFB correction improves radar data quality (Rabiei and Haberlandt, 2015), it is known to underestimate rainfall in some situations (Chumchean et al., 2006). Seo and Breidenbach (2002) suggest a method to correct spatially varying non-uniform bias in radar estimates by considering a small bin within the radar domain. The authors termed this method as a local bias correction method where locally varying bias is corrected instead of MFB (Seo et al., 2003). Based on the number of rain gauges and their distance from the radar, Chumchean et al. (2006a) present a method to update the current MFB estimate by applying a Kalman filter.

The application of bias correction depends mostly on the availability and quality of gauge data (Seo et al., 2003). In real time, the number of rain gauges available are often very small. Therefore, spatial averaging with gauged locations is required to apply this method to the ungauged region (Seo and Breidenbach, 2002; Steiner et al., 1999; Smith and Krajewski, 1991). Several radar and gauge merging methods have been proposed, such as ordinary kriging, cokriging, kriging with external drift (KED) (Berndt et al., 2014; Velasco-Forero et al., 2009; Sideris et al., 2014; Creutin et al., 1988), kriging with radar error (KRE) (also known as conditional merging) (Sinclair and Pegram, 2005) and wavelet analysis (Kalinga and Gan, 2012). Among all tested kriging techniques, KED often yields the best results (Haberlandt, 2007; Delrieu et al., 2014; Jewell and Gaussiat, 2015). The common assumption in all these techniques is that the gauge rainfall is the primary true source and the radar data is auxiliary information that can be used to improve the spatial interpolation (Rabiei and Haberlandt, 2015; Goudenhoofdt and Delobbe, 2009). This assumption is generally required because of the uncertainties and errors that result from converting the radar reflectivity to rainfall intensity. It is commonly accepted that the most useful information from the radar is the spatial pattern of the rainfall intensity rather than its magnitude (Méndez-Antonio et al., 2009). Rain gauges are more accurate, but conversely their measurements are only representative of a very small area (Goudenhoofdt and Delobbe, 2009; Martens et al., 2013). Furthermore, even if there are uncertainties in radar rainfall estimates, it does contain useful information about the temporal distribution of rainfall (Martens et al., 2013; Shucksmith et al., 2011). In this paper, we argue that if the errors in the rainfall field derived from gauges and radar can be accurately quantified, this information can be used to efficiently combine the two products without discarding the intensity information from the radar. This paper presents a method for combining spatially interpolated gauge rainfall with a radar rainfall estimate. Such combination is accomplished without making assumptions on the relationship between radar reflectivity and gauge rainfall. Furthermore, it considers the dependence between the radar and gauge estimates and thereby shows improvement over either the radar or gauge estimates taken individually.

In merging the radar and gauge products, there are parallels with recent work in combining multiple climate models or seasonal forecasts (Chowdhury and Sharma, 2009). One of the important findings from these studies is that dynamic weighting of the models (i.e. where the combination weights change with time) provides superior performance compared to static weighting schemes (Chowdhury and Sharma, 2010; Devineni and Sankarasubramanian, 2010). We therefore propose dynamic weighting to merge the radar and gauge data, which to our knowledge is a new contribution to the field. Dynamic weighting requires estimates of the error in each of the models at every location and every time step. The proposed method weights two different sources of information (radar and gauge estimates) based on their temporal distribution of errors without giving priority to one over another. We therefore propose an improved radar-rainfall relationship that calculates the uncertainties for different rainfall intensities.

Radar-rainfall relationships are very complex. The Z-R relationship depends on the drop size distribution of the rainfall as well as the rainfall regime and geographical location (Lee and Zawadzki, 2005; Steiner et al., 2004; Hazenberg et al., 2011). For example, Marshall and Palmer (Marshall and Palmer, 1948) found that, theoretically, reflectivity and rainfall intensity should be proportional to the 6th and 3.7th moments of the raindrop diameter respectively. Hence, radar reflectivity is more sensitive to rain drop diameter than to rainfall rate. Moreover, it has been observed that the Z-R relationship can be non-injective, such that a reflectivity value can correspond to samples having different drop size distributions and rainfall intensities (Ochou et al., 2011; Uijlenhoet, 2001). While DSDs obtained by disdrometers can be used for obtaining the Z-R relationship (Prat and Barros, 2009; Verrier et al., 2013), these measurements are not available in many parts of the world (Mapiam et al., 2009; Hasan et al., 2014) and statistical calibration of the Z-R relationship is required. The commonly used power-law, with only two free parameters (A and b), is unable to capture this complexity. To circumvent this limitation and make the best use of available records of radar reflectivity and ground rainfall, we propose a nonparametric method to model the full complexity of the Z-R relationship.

Nonparametric methods have been found to be efficient in a number of hydrologic applications including streamflow simulation (Sharma et al., 1997; Sharma and O'Neill, 2002) and synthetic rainfall generation (Oriani et al., 2014). Villarini et al. (Villarini et al., 2008) calculated nonparametric radar rainfall uncertainties in a study involving a dense gauge network and radar measurements. They formed a conditional expectation function to estimate the expected areal averaged ground rainfall for a given radar rainfall estimate. It was found that the nonparametric approach had similar performance to copula-regression estimates with the advantage of being able to better adapt to local variations in the data. A downside is the sensitivity to outliers, particularly at the smallest timescales (5–60 min) where there was a lot of variability in the data. A nonparametric method for converting radar reflectivity into rainfall was proposed by Calheiros and Zawadzki (1987). It assumes the same probability for gauge measured rainfall and radar-derived estimates (Rosenfeld et al., 1993; Seed et al., 1996). This probability matching method (PMM) overcomes limitations related to the sampling volume. In addition, PMM also eliminates collocation and timing errors because it does not consider the actual timing when the Z-R pair occurred (Piman et al., 2007). Later, the Window Probability Matching Method (WPMM) (Rosenfeld et al., 1994) was developed, which alleviates limitations of the PMM method by considering homogeneous rainfall regions. In the WPMM, the probability distribution of reflectivity is matched with gauge rainfall over small spatial extents and time windows. Finally, the Window Correlation Matching Method (WCMM) (Piman et al., 2007) was developed by introducing a space window to correct timing and collocation errors. The WPMM and bias-corrected regression based on Z-R relationship have similar skill (Rosenfeld and Amitai, 1998) in the estimation of rainfall accumulation. However, the Z-R approach overestimates low rainfall intensities and underestimates high rainfall intensities compared to WPMM. The PMM has a limitation regarding estimation of high rainfall rates. The maximum rain rate predicted by the PMM cannot exceed the observed maximum rain rate, therefore Seed et al. (1996) suggested using a least square regression based Z-R relationship. Piman et al. (2007) found that WCMM method provides better rainfall estimates of mean aerial and point rainfall than PMM and WPMM. However, none of these methods consider the joint distribution of reflectivity and rainfall and the inter –association between reflectivity and rainfall pairs. Another limitation of these methods is the limited extrapolation of rainfall when larger than observed reflectivity is recorded. The proposed kernel-based nonparametric method (NPR) is in some ways an extension of PMM that address these limitations, except that a conditional (and not a quantile matching) approach is used. The proposed NPR method uses the bandwidth of reflectivity and rainfall pair instead of utilizing all the reflectivity – rainfall pair which is the major limitation of least square regression.

In this paper, we propose a nonparametric relationship between radar reflectivity and the expected ground rainfall estimate. The resulting radar rainfall estimate is then combined with an interpolated rain gauge field using a dynamic weighting scheme. The combination addresses the known sensitivity of nonparametric approaches to limited record lengths, as the combination will automatically assign a greater weight to the approach that exhibits a lower error.

Interpolation of rain gauge measurements onto a regular grid can be achieved in a number of ways. Previous studies have investigated inverse distance weighting (Kurtzman et al., 2009; Hwang et al., 2012), Thiessen polygons (Okabe et al., 2009), nearest neighbour (Isaaks and Srivastava, 1990), thin plate smoothing splines (Hutchinson, 1998), genetic algorithms (Chang et al., 2005; Huang et al., 1998), kriging (Cressie, 1988; Goovaerts, 2000), and conditional bias penalized kriging (Seo, 2013; Seo et al., 2014). Among these methods, kriging is most widely used. It uses the information from nearby locations to estimate the target parameter at a particular location. However, there are several drawbacks in kriging related to underlying assumptions of Gaussianity, and the difficulty in accommodating high-order types of non-stationarity such as changing variance across the spatial domain (Bárdossy and Li, 2008). Another problem in the context of rainfall interpolation is that variograms are affected by skewed distributions and outliers (Li et al., 2011). Copulas have been shown to overcome these problems. In particular, they allow the spatial dependence between random variables to be captured from their univariate distributions, excluding the information from marginal distributions. Moreover, copulas are less sensitive to measurement outliers and do not require transformations into a Gaussian space, which can result in intractable biases for high-order properties (Bárdossy and Li, 2008; Bárdossy, 2006). However, as is the case with most approaches, subjective parameter choices within a Copula framework can lead to model structural uncertainty, leading to overly “rough” or “smooth” spatially interpolated rainfall. A way around this was recently proposed by Wasko et al. (2013), who presented a combinatorial algorithm to form a spatial rainfall estimate that consistently outperforms a stand-alone Copula. This Copula-based combinatorial spatial rainfall estimation procedure has been used here as a means of interpolating gauge rainfall data throughout this paper. It is important to note that the combination approach does not rely on this choice and could be implemented with any other interpolation method as long as estimates of variance in the fitted surface are available.

In summary, this research aims to answer two main questions with respect to the merging of radar and rain gauge data. Firstly, can a nonparametric approach provide better estimates than a traditional gauge adjusted Z-R relationship? Secondly, what is an effective method of combining the radar and gauge based estimates that can account for their respective strength and weakness? The rest of this paper is organized as follows. The proposed methods are presented in Section 2. Section 3 describes the study area and the data used. The rainfall estimation results are discussed in Section 4. Finally, Summary and conclusions are presented in Section 5.

2. Methodology

This section describes the proposed methods to merge radar and gauge estimates. First, we discuss the nonparametric rainfall estimation method (NPR). The copula-based rain gauge interpolation (CSI) method is then presented followed by details of the dynamic combination of both products.

2.1. Radar rainfall relationships

2.1.1. Non parametric rainfall estimation (NPR)

The NPR method aims to estimate ground rainfall for a given reflectivity by using a parametric kernel function. The application of the NPR method requires the kernel bandwidth and the conditional covariance matrix to be estimated from past observed rainfall and reflectivity data. Then, the conditional mean and conditional weight for each kernel are estimated. For a given radar reflectivity, the local weighted average of the conditioned kernels gives the expected rainfall.

To illustrate the NPR method, we consider the problem of estimating ground rainfall (R_{NPR}) from the given radar reflectivity (Z). The rainfall and reflectivity are in units of mm/h and dBZ respectively. The past observed radar rainfall record contains rainfall (r_i) and corresponding reflectivity (z_i) for each time step i, where $i = 1,\ldots n$. The conditional probability density of R_{NPR} given Z can be written as (see Sharma et al., 1997 for details):

$$\hat{f}(R_{NPR}|Z) = \frac{1}{n}\sum_{i=1}^{n}\frac{1}{(2\pi\lambda^2 S_c)^{1/2}} w_i \exp\left(-\frac{(R_{NPR}-b_i)^2}{2\lambda^2 S_c}\right) \quad (1)$$

where S_c is the conditional covariance formed on the basis of past observed rainfall-reflectivity pairs that measure the spread of the conditional probability density. S_c is defined as:

$$S_c = S_{RR} - \frac{S_{RZ}^2}{S_{ZZ}} \quad (2)$$

where S_{RZ}, S_{RR} and S_{ZZ} are sample covariance and respective variances of the two variables; λ is the bandwidth, adopted as the Gaussian reference bandwidth for standardised data (see Silverman, 1986 for details) and is estimated as:

$$\lambda = 1.06n^{-1/5} \quad (3)$$

Next, b_i is the conditional mean associated with the ith kernel. It is equivalent to the projection of the observed response related to that kernel (r_i) along the slope of a linear regression fit as dictated by the deviation ($Z - z_i$):

$$b_i = r_i + (Z - z_i)\frac{S_{RZ}}{S_{ZZ}} \quad (4)$$

w_i is the conditional weight for each kernel or the fractional probability that a kernel contributes to the overall makeup of the conditional probability density of R|Z:

$$w_i = \frac{p_i}{\sum_{i=1}^{n} p_i} \quad (5)$$

where $p_i \propto \exp(-\frac{(Z-z_i)^2}{2\lambda^2 S_{ZZ}})$

The expected rainfall for a given radar reflectivity can then be estimated as the mean of the conditional PDF in (1):

$$R_{NPR} = \sum_{i=1}^{n} (w_i b_i) \tag{6}$$

In the above description, the Gaussian reference bandwidth is assumed for simplicity. Alternate bandwidths that vary depending on the local probability density associated with each data point can be formulated based on the approach proposed by Sharma et al. (1998). While the formulation above uses a single conditioning variable (Z), one could include additional covariates such as gradients in the reflectivity field in x and y directions. Extensions of the conditional kernel density estimate presented above to include additional covariates would then require use of partial weights that scale the Euclidean distances in Eq. (5) and prescribe the importance each covariate has to the response (Sharma and Mehrotra, 2014). In the NPR method, the local weighted average is calculated with more weight being given to the values closer to target reflectivity and less weight for the values further away from target reflectivity. Therefore, the NPR method is expected to provide better rainfall estimate compared to a parametric radar-gauge relationship. The method is sensitive to the past observed data set and therefore it is necessary to have enough reflectivity-rainfall pairs to obtain statistically robust rainfall estimates. However, the NPR method can extrapolate based on $(Z-z_i)$ and the slope S_{RZ}/S_{ZZ} as per Eq. (4). Readers are referred to Sharma et al. (1997) for further details and illustrations of how conditional probability density estimates are derived from the joint PDF. The NPR method is developed using non zero reflectivity – gauge rainfall pairs. The threshold for reflectivity is 15 dBZ and for gauge rainfall is 0.2 mm/h. The data-pairs with either value less than the threshold were excluded to minimize the error due to noise at low intensities. While the conditional expectation can assume negative values (in which case they would be set equal to zero), no such cases were encountered in the data that was used in our study.

2.1.2. Parametric rainfall estimation (Z-R relationship)

In the results presented later, a traditional Z-R relationship has also been fitted to the available radar and gauge data for comparison to the new NPR method (details are provided in Section 3). This was achieved by pooling all data available and using a linear regression to determine the value for the A parameter, holding the b parameter constant at the operational value of 1.53 (Hasan et al., 2014). Although the operational Z-R relationship could have been used, this would not have provided a valid comparison for the NPR method since the operational relationship is obtained using a different time period. There are some differences in the resulting radar gauge relationship ($Z = 183.87\ R^{1.53}$) compared to the operational one ($Z = 194\ R^{1.53}$) for this radar, which are likely due to differences in the data length and time window. It is worth noting that the operational relationship is also based on a gauge-radar adjustment. The use of a fixed b parameter follows from recommendations in Henschke et al. (2009). In the remainder of this paper, this fitted radar - gauge relationship (designated as "parametric Z-R") is used to compare the performance of the proposed NPR and combination methods.

2.2. Copula-based rain gauge interpolation (CSI)

The gauge data needs to be interpolated on to the same pixels as the radar to combine the gauge and radar rainfall estimates. As discussed in the Introduction, a copula based spatial interpolation (CSI) method is chosen to achieve this. The primary focus of this paper is not to develop a new spatial interpolation method but to apply the combined copula interpolation algorithm developed by Wasko et al. (2013) using the spatial copula toolbox (Kazianka, 2013a) which we call the copula based spatial interpolation (CSI). The CSI is used to create a grid of rainfall values at all the pixel locations for each 30 min periods considered (more details on the data are given in the next section). In CSI, a rainfall estimate at each radar pixel is interpolated using copula parameters estimated using all available data (global) as well as a local neighbourhood. The global and local estimates are then combined using the errors at each unknown location (Wasko et al., 2013) to produce a rainfall estimate at that location. This is repeated for all pixel locations and for all individual 30 min periods . In this approach, the rainfall at any particular radar pixel is interpolated using the gauge observations at that time step. For the purposes of testing the CSI method, leave-one-out cross-validation is used (Goovaerts, 2000). In this approach, the rainfall at any pixel with a coincident rain gauge is interpolated by ignoring the gauge observation at that particular pixel and interpolating the rainfall using the remainder of the gauge observations at that time step. Readers are referred to Kazianka (2013b) and Wasko et al. (2013) for further details of the copula-based combinatorial approach used.

It should be noted that the weight estimation process in this study, while having some similarities to kriging based methods such as KED and conditional merging (Severino and Alpuim, 2005), is significantly different in its makeup and form. The proposed method weights two different estimation approaches (NPR and copula-based interpolation). The weight is computed based on the temporal distribution of radar and gauge estimation errors, instead of the spatial distribution of radar and gauge estimation errors of individual rainfall periods. The conditional merging method performs a spatial interpolation on the radar rainfall which is not the case here. Moreover, the number of gauge measurements available has a significant effect on the variogram and the merged estimates (Habib et al., 2001). In contrast, our combination weight estimation process is independent of the gauge density which only affects the CSI estimates in a way that is similar to kriging. While it is possible to replace the CSI estimates with any of the kriging based methods discussed above, this is not attempted here and is recommended for future research.

2.3. Combination method

At each radar pixel, we now have two rainfall estimates, the first from the NPR method and the second from the CSI method. The final rainfall is estimated by combining the CSI and NPR values according to the confidence that we have in each. This confidence comes from the past observed estimation accuracy of each method and is expressed as weights. The two sources of information are merged using a dynamic combinatorial algorithm with weights that vary in both space and time. The weight for any specific period is calculated based on the error covariance matrix that is formulated from the radar and spatially interpolated rainfall errors of similar reflectivity periods in a cross-validation setting. The application of the combination method to any particular pixel requires the past observed records of NPR and CSI estimation error at that pixel or near that pixel. The overall process is illustrated in Fig. 1.

The weights are estimated using leave one out cross-validation. The weight for any 30 minute periods is calculated based on the error covariance matrix constructed from similar previous reflectivity measurements at the nearest radar pixel with a coincident rain gauge. The similar reflectivities are identified through the application of a nonparametric k-nearest neighbour (KNN) approach to the past observed data (Lall and Sharma, 1996). The covariance matrix of errors is formulated from the k-similar periods in the past observed dataset, not including the current NPR and CSI estimates. In the combination algorithm, the sum of weights is equal to one and weights cannot be negative (Timmermann, 2006). The final rainfall

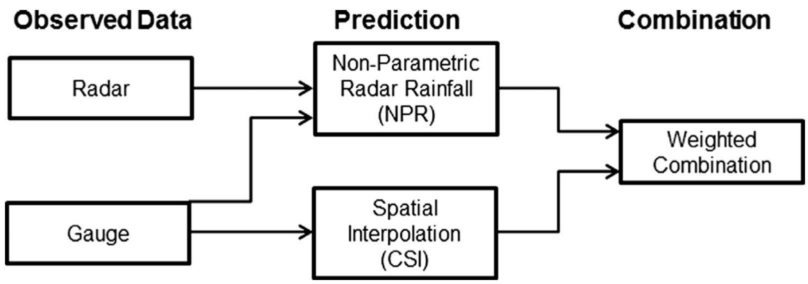

Fig. 1. Flowchart for weighted combination method.

estimate at a particular location and time is the weighted sum of the NPR and CSI estimates.

The combination method is illustrated through the following example. Suppose that we want to find the weights for each of the CSI and NPR methods for an observed reflectivity $Z_{t,x}$ at location x and time t. The corresponding rainfall estimates from the CSI and NPR methods are $R_{CSI,t,x}$ and $R_{NPR,t,x}$ at the same location and time. We also have the sets of all observed, CSI and NPR estimates from the nearby gauged location for n times, which we call $\mathbf{R_h}$, $\mathbf{R_{CSI}}$ and $\mathbf{R_{NPR}}$ respectively. The idea is to find $\mathbf{W}$, which is a vector of two weights, W_{CSI} and W_{NPR}, where $W_{CSI} + W_{NPR} = 1$. The procedure adopted is as follows:

(1) Form the matrix $\mathbf{Y} = [\mathbf{Z_h} \quad \mathbf{R_h} \quad \mathbf{R_{CSI}} \quad \mathbf{R_{NPR}}]$ of past observed reflectivity ($\mathbf{Z_h}$), observed rainfall and the corresponding rainfall estimates from the CSI and NPR methods from the closest gauged pixel.

(2) The reflectivity periods that are similar to the observed reflectivity ($Z_{t,x}$) in the past observed records are estimated by calculating the smallest absolute distance (d_i) between Z_h and $Z_{t,x}$ in the matrix Y.

$$d_i = \min |Z_h - Z_{t,x}| \tag{7}$$

where, i is the ith element of vector Z. The distances d_i are sorted in ascending order and the first k periods are selected from matrix $\mathbf{Y}$.

(3) For each of the k periods, calculate the error for CSI and NPR methods ($\mathbf{e}_{\mathrm{CSI}}$ and $\mathbf{e}_{\mathrm{NPR}}$) as the difference between $\mathbf{R_h}$ and $\mathbf{R_{CSI}}$ or $\mathbf{R_{NPR}}$ respectively.

$$\mathrm{e_{CSI}} = \mathrm{R_h} - \mathrm{R_{CSI}} \tag{8}$$

$$\mathrm{e_{NPR}} = \mathrm{R_h} - \mathrm{R_{NPR}} \tag{9}$$

(4) Find the covariance matrix of the estimation errors, $\mathbf{\Sigma_e}$. Since we have two methods, the size of the covariance matrix is 2 by 2 with the diagonals representing the variance of the errors over the k neighbours and the off-diagonals the covariance of the errors from the two methods.

$$\sum\nolimits_e = \begin{bmatrix} S_{11} & S_{21} \\ S_{12} & S_{22} \end{bmatrix} = \begin{bmatrix} \sigma^2{}_{\mathrm{CSI}} & \rho\sigma_{\mathrm{CSI}}\sigma_{\mathrm{NPR}} \\ \rho\sigma_{\mathrm{CSI}}\sigma_{\mathrm{NPR}} & \sigma^2{}_{\mathrm{NPR}} \end{bmatrix} \tag{10}$$

where, $\sigma^2{}_{\mathrm{CSI}}$ and $\sigma^2{}_{\mathrm{NPR}}$ are the variance of the estimation errors, $\mathbf{e}_{\mathrm{CSI}}$ and $\mathbf{e}_{\mathrm{NPR}}$ respectively, ρ is the correlation between estimation errors.

(5) The dynamic weights (W′) for combining CSI and NPR estimates can be obtained by minimizing the quantity in (11) subject to the constraint that the weights add up to unity.

$$\min \left(\mathrm{W}' \sum_e \mathrm{W} \right) \quad \text{such that} \quad \mathrm{W}' l = 1 \tag{11}$$

where, $\mathrm{W}' = [\mathrm{W_{CSI}} \ \mathrm{W_{NPR}}]$, $\boldsymbol{l}$ is a m x 1 column vector of ones where m denotes the number of methods with $m = 2$ in this case, the weights being constrained to lie between 0 and 1. Readers are referred to Timmermann (2006) and Khan et al. (2014) for further details concerning the derivation of Eq. (11).

(6) The final combined rainfall estimate is then the weighted average of the different methods:

$$\mathrm{R_{COMBINATION}} = \mathrm{W_{CSI}R_{CSI,t,x}} + \mathrm{W_{NPR}R_{NPR,t,x}} \tag{12}$$

The covariance matrix at any particular location and time is unique for each rainfall observation. The main free parameter in this method is the number of neighbours to use in calculating the error covariance matrix. In this case, 200 neighbours are selected. The main sources of uncertainty in the combination method arise from how the weights for the two methods are determined. In this study, a k-nearest neighbours approach was adopted. This means that the primary uncertainty is in the number of neighbours to be used in estimating the covariance matrices of the gauge and radar error estimates. The adopted value of 200 neighbours was chosen following a sensitivity analysis of the relations of the RMSE to the number of neighbours. As the number of neighbours increases, the errors rapidly decrease until about 100 neighbours are used. After this the rate of decrease slows until the relationship flattens with about 200 neighbours. The adopted value of 200 was therefore chosen, in agreement with Khan et al. (2014). This value constitutes a trade-off between large biases and the need for too much data. In our study, most of the gauge locations contain around 300 observations, and very few of them contain less than 200 observations. At the few locations with less than 200 data points, data from the nearest gauge are used.

2.4. Quality metrics

The errors are assessed using the root mean square error (RMSE), mean absolute error (MAE), median absolute error (MedianAE), bias and mean relative error (MRE) (Bennett et al., 2013; Wang et al., 2012). MedianAE denotes the median of absolute error (AE). Rainfall often has a highly skewed distribution. Hence, the RMSE and MAE error estimates will be strongly influenced by the highest rainfall rates. This is why we have also chosen to use MRE and MedianAE, which are expected to be less influenced by the magnitude of rainfall (Wasko et al., 2013). These measures are formulated as follows:

$$\mathrm{RMSE} = \sqrt{\frac{1}{n}\sum_{i=1}^{n}(\mathrm{R_{est}} - \mathrm{R_g})^2} \tag{13}$$

$$\mathrm{MAE} = \frac{1}{n}\sum_{i=1}^{n}|\mathrm{R_{est}} - \mathrm{R_g}| \tag{14}$$

$$\mathrm{AE} = |\mathrm{R_{est}} - \mathrm{R_g}| \tag{15}$$

$$\mathrm{Bias} = \frac{\sum_{i=1}^{n}\mathrm{R_{est}}}{\sum_{i=1}^{n}\mathrm{R_g}} \tag{16}$$

$$\mathrm{MRE} = \frac{1}{n}\sum_{i=1}^{n}\frac{|\mathrm{R_{est}} - \mathrm{R_g}|}{\mathrm{R_g}} \times 100\% \tag{17}$$

The RMSE is a commonly used performance measure that provides the overall skill measure of a method. The overall systematic error of a method is assessed by bias whereas, Conditional Bias (CB) measures how an estimated rainfall differs from the gauge estimate (Habib et al., 2008; Ciach et al., 2000). The conditional bias conditioned to rainfall rate and radar reflectivity are formulated as follows:

$$CB_g(a < R_g \leq b) = \frac{\sum_{i=1}^{n} R_{est|}|(a < R_g \leq b)}{\sum_{i=1}^{n} R_g|(a < R_g \leq b)} \tag{18}$$

$$CB_R(a < dBZ \leq b) = \frac{\sum_{i=1}^{n} R_{est|}|(a < dBZ \leq b)}{\sum_{i=1}^{n} R_g|(a < dBZ \leq b)} \tag{19}$$

where R_g represents gauge rainfall and R_{est} represents estimated rainfall estimated using one of the four methods, CB_g is the conditional bias conditioned to gauge rainfall rate, CB_R is the conditional bias conditioned to radar reflectivity and a, b represent the lower and upper bounds of the moving window.

3. Study region and data

The NPR, CSI and combination methods have been tested over the Sydney region where the Australian Bureau of Meteorology operates the Terrey Hills radar and a relatively dense network of tipping bucket rain gauges. The S-band Terrey Hills radar covers a 256 km by 256 km region. It is a Doppler radar with a wavelength of 10.7 cm and a bandwidth of 1°. The radar precipitation estimates have a temporal resolution of 6 min and spatial resolution of 1 km. Of the approximately 65,000 km^2 area covered by the radar, 55% is on land. The remainder of the domain, which is over the Pacific Ocean, has been disregarded from the analyses due to the absence of gauge observations. Data from November 2009 to December 2011 (two years) were used to analyse the performance of the proposed methods. The gauge data was collected from the Australian Bureau of Meteorology and Sydney Water and the radar data was obtained from the Australian Bureau of Meteorology.

The rainfall periods were selected by visual inspection of the radar images using the radar rainfall software Mapview (Seed and Jordan, 2002) and resulted in 1442 half-hour rainfall periods available for the analyses. Noise and hail effects (Chumchean et al., 2004; Chumchean et al., 2006b) were avoided by limiting the reflectivity values to between 15 dBZ and 53 dBZ. In the Sydney area, the climatological freezing level is 2.5 km (Chumchean et al., 2003). Therefore, bright band effects were avoided by selecting 1.5 km Constant Altitude Plan Position Indicator (CAPPI) reflectivity data. To minimise errors at very low rainfall intensities, a minimum threshold of 1 mm/h was adopted (Chumchean et al., 2006a; 2004).

Within the study region, there are 282 tipping bucket gauges with bucket sizes of either 0.2 or 0.5 mm. The locations of these gauges are shown in Fig. 2a, overlaid on the topography of the study region. The gauge density is high within 50 km of the radar and most of the gauges are located near the coast and to the south of the radar. Further inland, gauge densities are lower, in particular in the Blue Mountains where elevations reach up to 1600 m above sea level. Mean annual rainfall, based on a standard 30-year climatology (1961–1990), is presented in Fig. 2b. There is a strong east-west rainfall gradient with the driest areas located at the foothills of the Blue Mountains and higher rainfalls observed on the tops of the ranges. The area of highest rainfall is found to the south of Sydney in the Wollongong area and is due to the Illawarra Escarpment where the land rises steeply close to the coast.

4. Results

The performance of the different rainfall estimation methods is presented in this section, looking at aggregated results and temporal and spatial variations. The variation of the results with respect to rainfall rate and reflectivity is then presented.

4.1. Performance of the proposed methods

For each half-hour rainfall period, we have calculated the radar rainfall using the parametric Z-R and NPR methods and the gauge rainfall using the CSI method. For each period, the NPR and CSI rainfall estimates are then merged using the dynamic combination approach. The performance of all four methods (parametric Z-R, NPR, CSI and combination) are evaluated by comparing them with the gauge observations and are presented in Table 1.

The results displayed in Table 1 (aggregated over all 1442 rainfall periods) show that the NPR method is superior to the parametric Z-R method, with improvements in four error statistics (RMSE, MAE, MedianAE and MRE). Additional tests (not shown here) have been carried out for coarser timescales (60, 90 and 120 min). These tests indicate that the NPR method gives slightly better rainfall estimates at larger time scales compared to the Z-R approach. Overall, the NPR performs better than the Z-R approach for all the timescales considered. The overall bias from the NPR method is similar to the parametric Z-R method. We suspect this could be due to the fact that the entire data is used in formulating the parametric Z-R, whereas this happens in a spatially distributed fashion in the case of the NPR. It should be noted that any bias larger than one indicates an overestimation of ground rainfall.

The uncertainties in the radar-rainfall relationships (both parametric and nonparametric) are clear when we compare the CSI results to the radar-derived ones. The CSI method has smaller MRE than both parametric Z-R and NPR methods. The best performance is obtained from the combination method, with improvements in four error statistics (RMSE, MAE, MedianAE and MRE). Compared to the parametric Z-R method, the NPR has improved RMSE by 10% while an even larger improvement (20%) is obtained using the combination method.

To illustrate the differences in the four methods, Fig. 3 compares the rainfall estimates for a single period on 01 November 2010 at 06:30 UTC. For small reflectivities the rainfall estimates are higher using the NPR method than with the parametric Z-R method, which is evident from the larger areas of light blue in Fig. 3b than in Fig. 3a. In contrast, for the highest reflectivities the NPR method leads to lower rainfall estimates compared to the parametric Z-R which is evident from the smaller number of red points in Fig. 3b than in Fig. 3a. For the gauge based CSI method, the non-zero measurements at gauges in the northeast and centre of the study area have led to quite different patterns in the rainfall than the radar estimates (Fig. 3c). To illustrate the dynamic weighting in combination method, we evaluated the estimation at the locations marked by A, B, C, D, and E shown in Fig. 3.The performance of the combination method depends on the weights of the participating methods. Around location A, the CSI method estimates high rainfall (Fig. 3c). At this location, the CSI and NPR methods have an average weight of 0.16 and 0.84 respectively. The combination method therefore reflects NPR and results in low rainfall amounts. The same happens at location B. The opposite scenario can be found at nearby radar locations around the Sydney region where gauge density is high and the average CSI weight is around 0.68. The Combination rainfall patterns are thus similar to the CSI method. As there is a fair number of gauges situated around the location D (in the Blue Mountain region), the average weight of CSI method will be higher at that location. The combination method thereby displays rainfall patterns similar to CSI and estimates intense rainfall for the particular period. At location E (near Newcastle region) both methods have similar weights. As both the methods estimate high rainfall at this location, the combination method just complies with them.

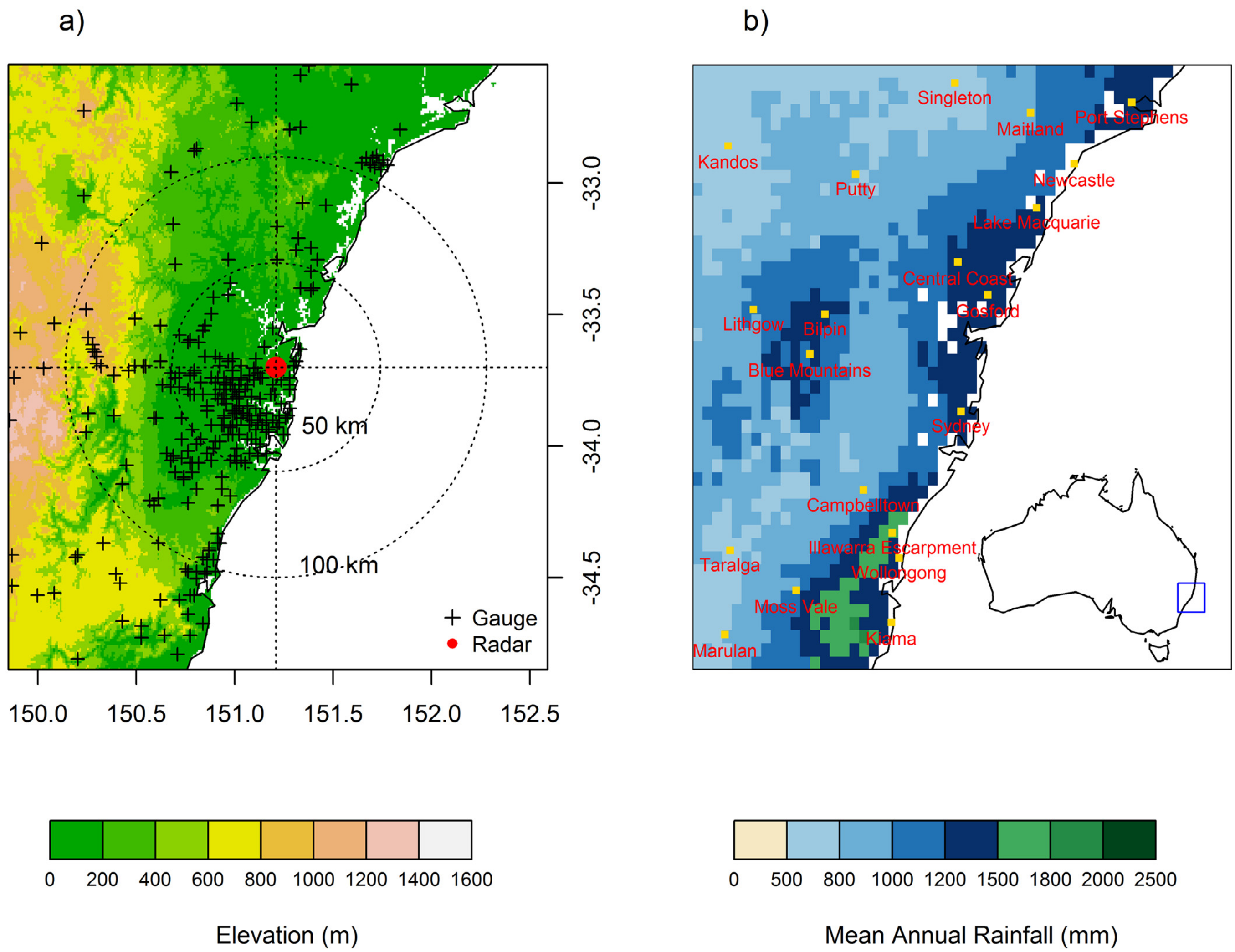

Fig. 2. (a) Topography of the study region showing the location of the Terrey Hills radar and rain gauge locations and (b) mean annual rainfall across the study domain.

Table 1
Performance measure of different estimation methods. Values in bold represent the best result in each category.

	RMSE (mm/h)	MAE (mm/h)	BIAS	MedianAE (mm/h)	MRE (%)
Parametric Z–R	4.37	2.64	**0.95**	1.53	76.08
NPR	3.97	2.41	**0.95**	1.43	73.44
CSI	4.17	2.22	0.79	1.10	59.85
Combination	**3.56**	**1.99**	0.86	**1.06**	**55.42**

There are few gauges in the western part of the domain and therefore there is limited information available to the CSI method in this area. This demonstrates the influence of the gauge network arrangement on interpolation methods, in particular relative to the spatial pattern of any particular storm period. The radar can provide more information on the spatial pattern and rainfall amounts in these poorly gauged areas. For this particular rainfall period, the error from the CSI method (Fig. 3c) is approximately equivalent to the NPR method. As seen for the overall results in Table 1, the combination method leads to the smallest error (Fig. 3d).

Another example of improvement for the combination method is shown in Fig. 4 for a single period on 21 July 2011 at 09:00 UTC. In Fig. 4, at location A, the NPR method shows intense rainfall whereas the CSI method shows moderate rainfall. As the weight is high for NPR, the combined figure shows the rainfall pattern similar to NPR, but with lower intensities. Locations near the radar have high gauge density. At location B, the combination method shows a rainfall rate similar to the CSI method as it has higher weight for this location. Locations in the Blue Mountains have fewer gauges and hence the CSI method has a larger weight compared to NPR. As a result, in D the combination method shows rainfall patterns driven by CSI. The NPR average weight is 0.60 around region C, resulting in the combination method rainfall pattern being similar to that from the NPR method.

As shown in Fig. 3, the spatial structure of the gauge network and the spatial patterns of rainfall periods lead to differences between the four methods. This spatial information is as important as the magnitude of the rainfall error in any hydrological analysis using the rainfall fields. In Fig. 5 the performance of each method across the study domain is presented. At each gauge location, the method that leads to the best results has been identified. In Fig. 5a

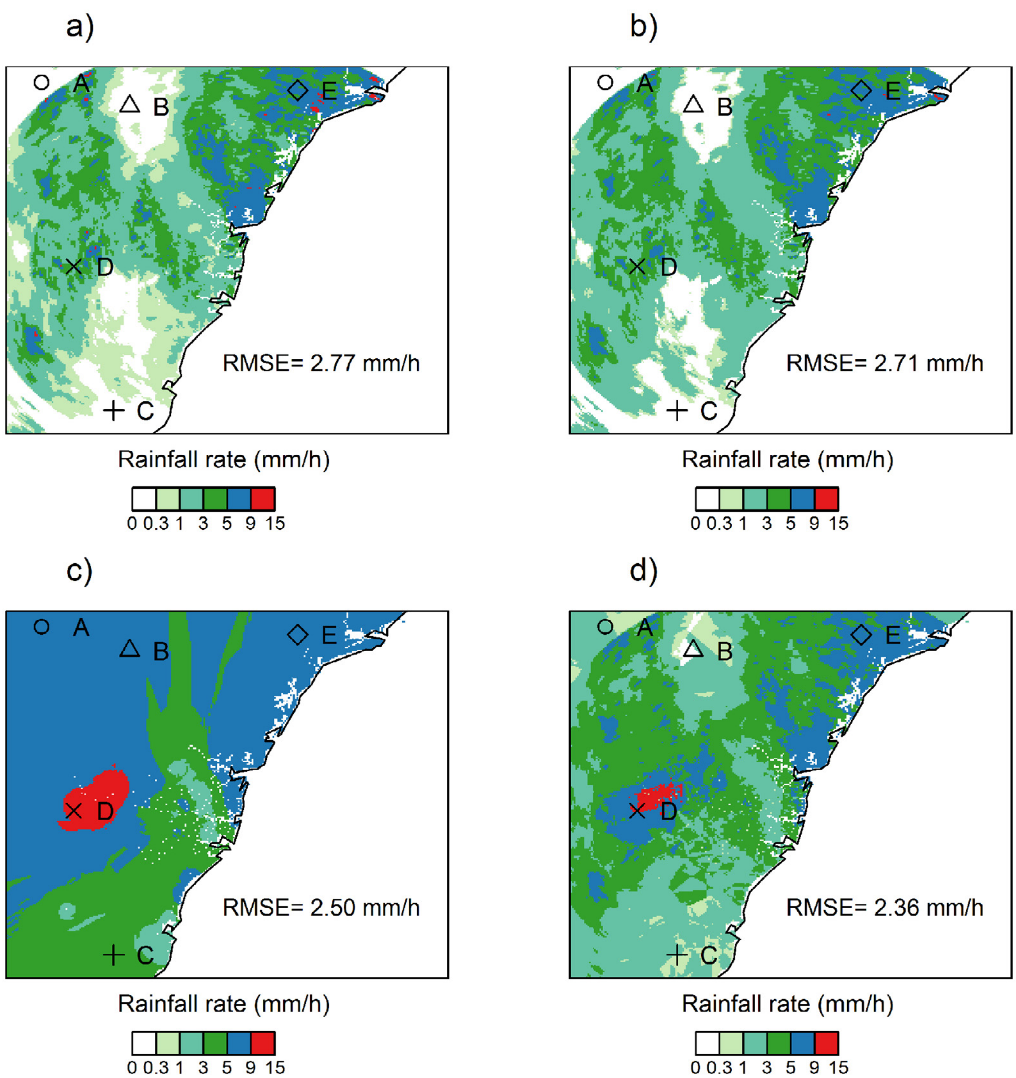

Fig. 3. Rainfall estimation for an individual storm period on 01 November 2010 at 06:30 UTC from (a) parametric Z-R (b) NPR (c) CSI and (d) combination method. (For interpretation of the references to colour in this figure legend, the reader is referred to the web version of this article.)

the parametric Z-R and NPR methods are compared. We can see that out of 282 gauge locations, the NPR method performs better than the parametric Z-R method at 246 gauge locations. For the same high reflectivity, the parametric method gives higher rainfall rates compared to the NPR method. This may be due to the relatively limited number of the Z-R pair dataset available for high reflectivities that is used to develop the NPR method. Therefore, in the high rainfall region the parametric method has a relatively smaller error compared to NPR.

The study region has a mixture of areas with high and low gauges densities. One high gauge density area is marked with “D” and one of the sparse gauge density area is marked with “S” in Fig. 5b. Also the performance of NPR with the gauge-based CSI estimation is shown in Fig. 5b. The NPR method provides more reliable estimates at 138 locations, particularly in the areas of low gauge density. The CSI method is reliable in the high gauge density area. This is to be expected given that the interpolation has much more information available in these areas.

Finally, all four methods are compared in Fig. 5c. The CSI method continues to lead to the best estimates in the densely gauged areas. The combined method produces better estimates in regions of lower gauge densities, showing the added value that the radar information can provide. The better performance at these locations leads to the overall smaller errors from this method as seen in Table 1.

Clearly gauge density is an important factor in determining the effectiveness of the different methods. To further assess this relationship, Table 2 separates the results according to the gauge density, with the regions shown in Fig. 6. The sparsely gauged area (S1) to the north west of Sydney has a density of 1 gauge per 612 km^2. The densely gauged region (D) has a gauge density of 1 gauge per 34 km^2. The gauge density over the full domain is 1 gauge per 127 km^2. We have calculated the RMSE for the parametric Z-R, NPR, CSI and combination methods across each of these three regions by comparing them with the observed gauge rainfall. Between the parametric Z-R, NPR and CSI methods, the NPR method has the smallest errors in the sparse region. For the dense region the CSI method minimises the errors as demonstrated previously in Fig. 5b. The combination method is found to be superior to all other methods for the sparse regions. The magnitude of the values presented in Table 2 confirms the efficiency of the NPR and combination method

In addition to the original sparse region (S1), we have investigated two other sparse regions with different numbers of rain gauges denoted by S2 and S3, as shown in Fig. 6. The total number of gauges in S3 region is around 3 times higher compared to S1

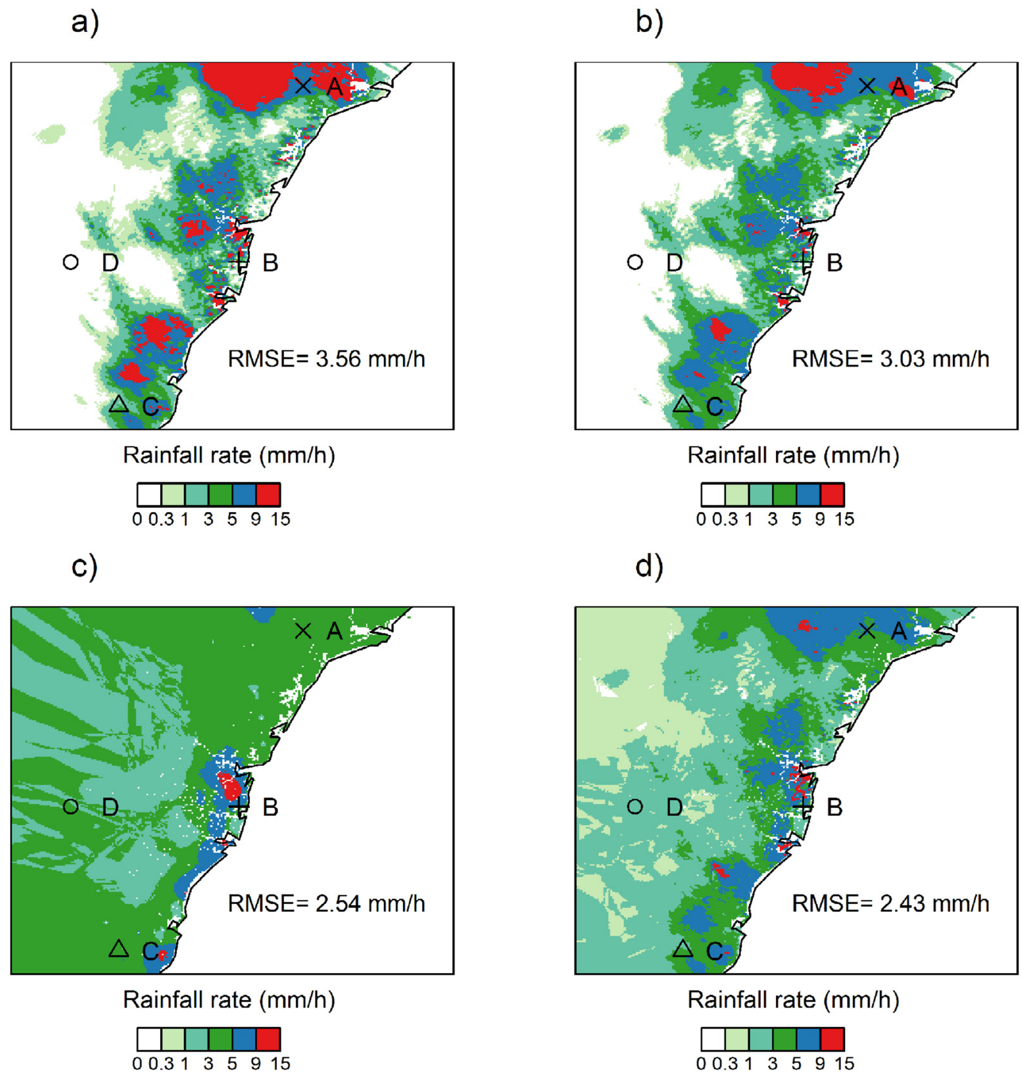

Fig. 4. Rainfall estimation for an individual storm period on 21 July 2011 at 09:00 UTC from (a) parametric Z-R (b) NPR (c) CSI and (d) combination method.

Table 2
RMSE (mm/h) across different regions. Values in bold represent the best result in each category.

	Sparse Region S1	Sparse Region S2	Sparse Region S3	Dense Region D	Whole Region
Parametric Z–R	4.01	4.22	4.74	4.18	4.37
NPR	3.46	3.58	4.44	3.82	3.97
CSI	4.54	3.98	5.01	3.76	4.17
Combination	**3.28**	**3.18**	**4.26**	**3.37**	**3.56**

region. From Table 2, it is clear that the conclusions remain the same even though we changed the sparse region. The NPR method performs better than the parametric Z-R method in terms of RMSE. Most importantly, the RMSE of combination method is the lowest among all other methods, whether we apply the combination method for sparse or dense region.

4.2. Spatial and temporal variation of weights

The results presented in the preceding sections have mainly considered the aggregate performance of each of the methods over all 1442 half-hourly rainfall periods. Also of interest is how the combination of the NPR and CSI method varies over all the periods. The dynamic weighting ensures that for any location the best method for a particular rainfall period is chosen. Information about how the weighting changes in time and space is valuable in providing further information about how the methods perform. The mean weight assigned to the NPR method at each gauge location is represented in Fig. 7a. In general, NPR weights are higher in the low gauge density regions. The kriging based merging method considers radar rainfall as a secondary information that improves the spatial interpolation of gauge rainfall estimates (Rabiei and Haberlandt, 2015; Goudenhoofdt and Delobbe, 2009). In contrast, the spatial and temporal variation of the NPR weights (Fig. 7) considers radar rainfall as potentially equally or more important than the gauge rainfall depending on the information content in the radar data. The exception is the area of gauges to the northeast of the radar where, consistent with the results shown in Fig. 5b, the CSI method leads to lower errors and therefore is more strongly weighted when combining both approaches.

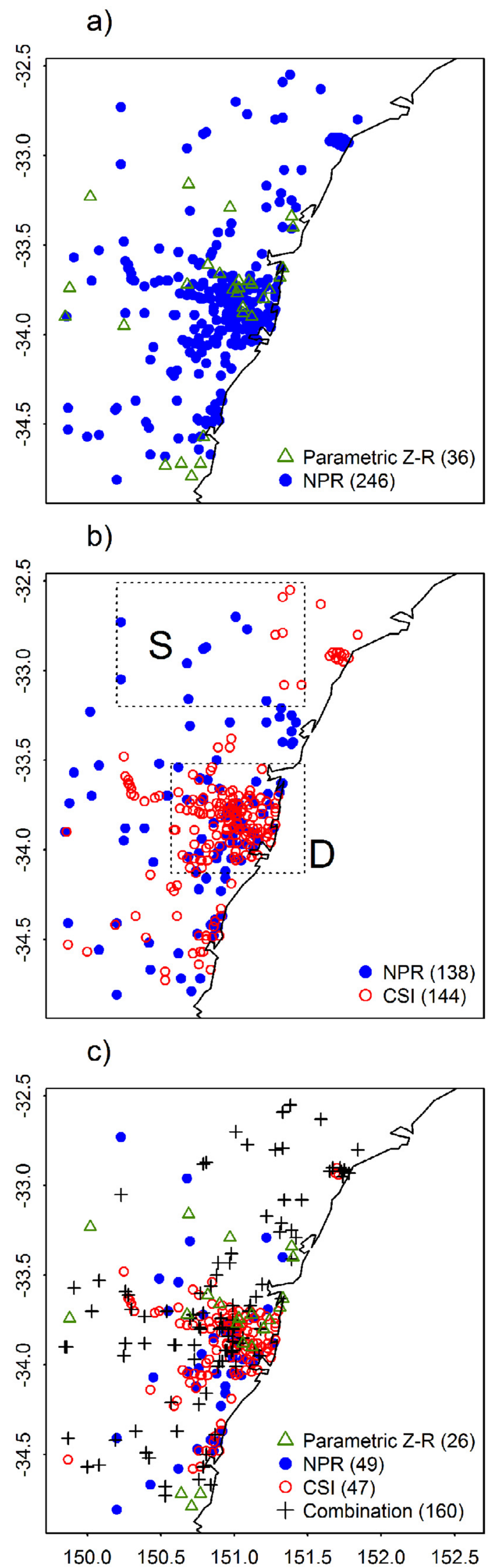

Fig. 5. Spatial representation of the best RMSE between (a) parametric Z-R and NPR (b) NPR and CSI (c) Parametric Z-R, NPR, CSI and combination method. Areas with high gauge density (D) and sparse gauge density (S) are shown in panel b).

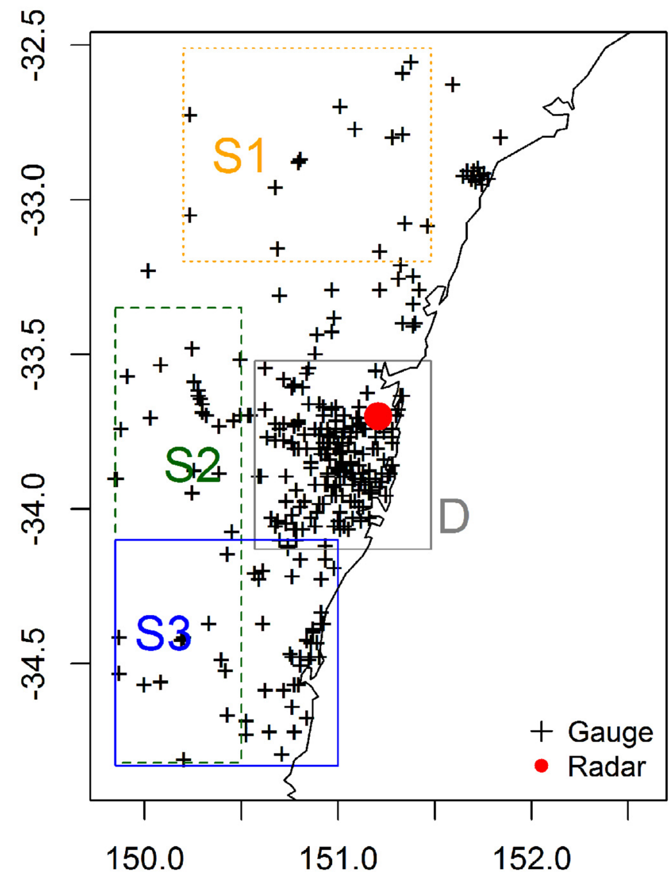

Fig. 6. Spatial representation of gauge density. The three sparse regions are denoted by S1, S2 and S3 respectively. Areas with high gauge density are denoted by (D).

We also have information on the temporal variation of the weights for any particular location. To demonstrate the utility of this information, three representative rain gauges X, Y and Z are highlighted in Fig. 7a. The gauge “X” was chosen to represent a high rainfall area, whereas gauges “Y” and “Z” are located in dense and sparsely gauged areas respectively. The mean weights and temporal variation of the NPR weights at these gauge locations are shown in Fig. 7b to d. At gauge X, the weight ranges from 0.38 to 0.80 (Fig. 7b) with a mean of 0.61. This gauge has relatively high rainfall but is located in a sparsely gauged region. At this location, radar provides better information on the magnitude of the rainfall totals compared to the gauge based estimates. Therefore, the weights are generally greater than 0.50.

At gauge Y the NPR weights are much lower, ranging from 0.11 to 0.40 with a mean of 0.32 (Fig. 7c). As there are many other gauges surrounding this gauge, the spatial interpolation is generally successful. Finally, at gauge Z, in the sparsely gauged region, the NPR weights range from 0.74 to 1.0 with a mean of 0.84. The mean NPR weights at other gauges in this area (Fig. 7a) are quite similar. When the weight of NPR method is equal to one, spatial interpolation does not provide any useful information. This occurs for periods during which spatial heterogeneity is particularly high over the domain. The CSI method does not capture highly spatially varied rainfall patterns well (such as when a high rainfall is observed adjacent to low rainfall in neighbouring gauges). The NPR estimates are calculated independently at each location and can therefore better capture rainfall periods with high spatial heterogeneity.

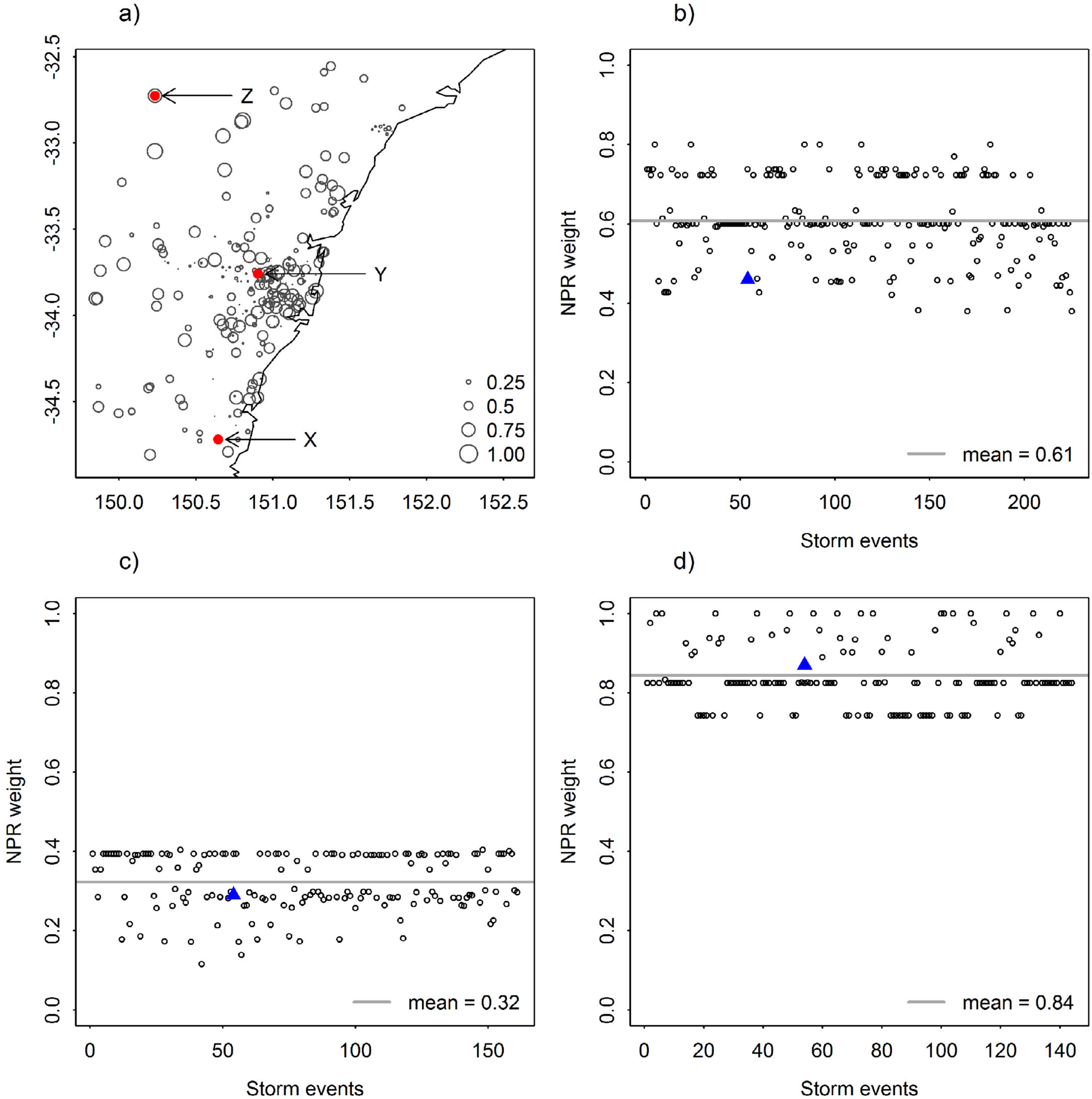

Fig. 7. The NPR mean weights (a) at different locations. The variation of the NPR weights for different storm periods are shown for (b) location X, (c) location Y and (d) location Z. The weights for the periods presented in Fig. 3 are shown in blue colour symbol (Fig. 5b–d).

4.3. Performance for different storm properties

The results presented above explore the performance of the different methods with respect to gauge density. In this section, we consider the relationship between the proposed methods and several rainfall characteristics such as rainfall rate and reflectivity. For each characteristic, the data set is binned into several classes.

The impact of rainfall rate on the performance of each of the estimation methods has been analysed by dividing the mean rainfall across the region into 4 mm/h bin size. For the different intensity rainfall periods, the CSI method leads to the lowest bias (Fig. 8). This is likely due to two reasons. The first is that there is less variation between adjacent gauges and hence the spatial interpolation is more successful. Secondly, the errors in the NPR method are quite high for small reflectivity periods (Fig. 8d). Additional data may assist in better defining the NPR relationship at these rainfall rates. Improvements from the NPR are evident by the larger reductions in bias than the RMSE. It is worth noting that the rainfall estimates from smaller and higher reflectivity bins using the parametric Z-R have the largest uncertainty (Fig. 8d).

For different rainfall rates, the combination method leads to the best performance, substantially reducing the MRE, RMSE and Bias

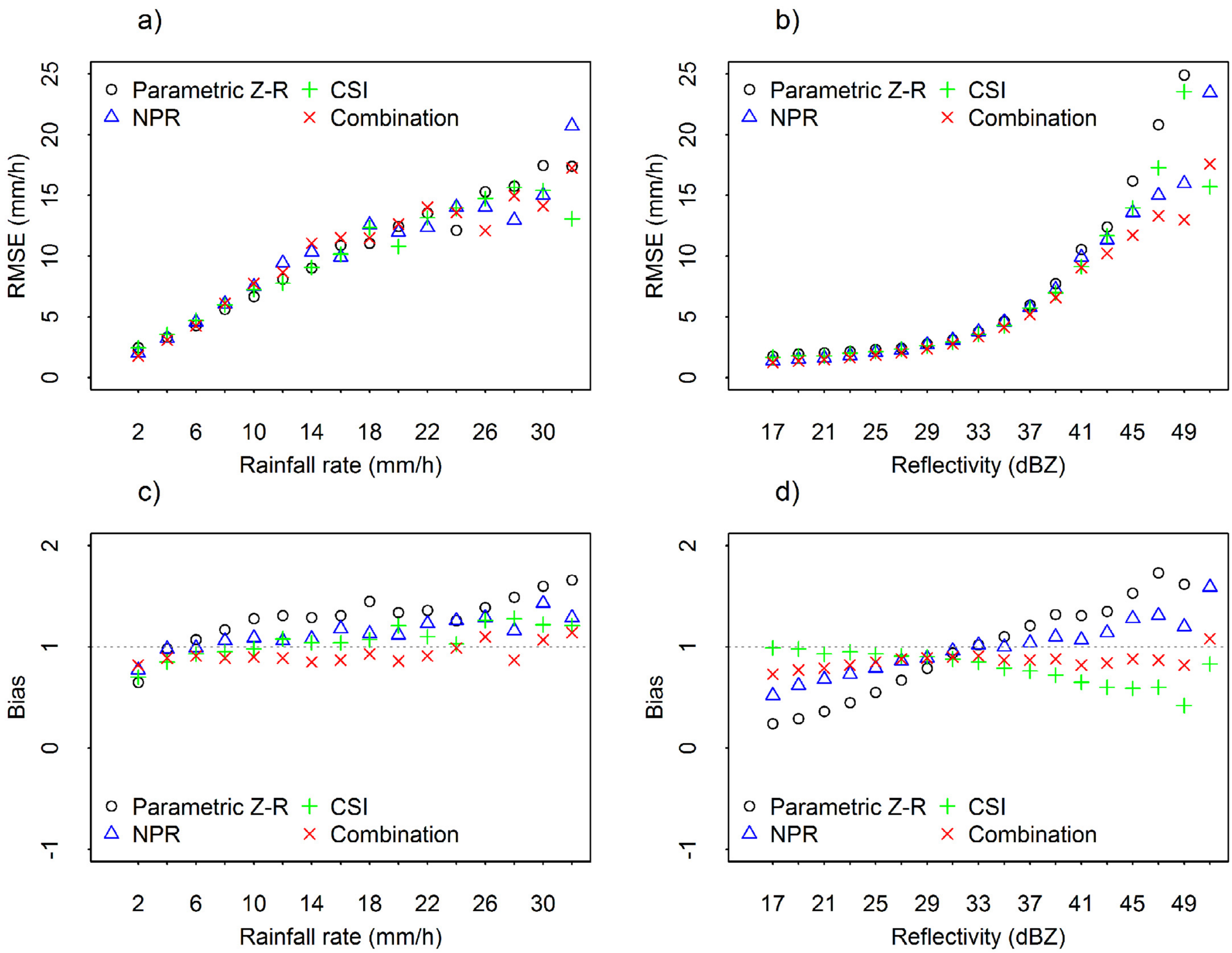

Fig. 8. The conditional performance measure of different estimation methods, conditioned to rainfall rate and reflectivity (a) RMSE conditioned to rainfall rate (b) RMSE conditioned to reflectivity (c) Bias conditioned to rainfall rate (d) Bias conditioned to reflectivity.

compared to using the radar alone and providing a modest improvement over the CSI method.

Similar to rainfall rate, we have divided the reflectivity into different bin size. For reflectivity, we have used a bin size of 2 dBZ. The results presented in Fig. 8 show that the NPR method performs better compared to the parametric Z-R method for all reflectivity bins. The results presented in Fig. 8 shows that high reflectivity bins lead to higher error for parametric Z-R compared to NPR. Similar to rainfall rates, the combination method leads to lowest RMSE for all reflectivity bins.

For higher rainfall rates, NPR leads to the lower estimation of ground rainfall compared to parametric Z-R. This is likely due to the lack of observed data points in the higher reflectivity band when we develop NPR from the past observed data set. Therefore, it is important to have a good number of past observed data to get an accurate rainfall estimate from all reflectivity bins using NPR. Improvements from NPR for the different rainfall rates are evident by the large reductions in RMSE and bias (Fig. 8). It is worth noting that the rainfall estimates from the higher reflectivity bins using parametric Z-R have the largest uncertainty (Fig. 8). However, we have also tested the combination method by incorporating the past observed records at the gauge of interest, rather than in the cross-validation setting used in the results section. If data from the gauge of interest are used then the uncertainty of the covariance matrix is smaller. The combination method provides better results with further improvement in RMSE of around 10%. If implemented in this way, the combination method can be used in real time to quality control gauge data by leaving out the measurement at a particular time step and comparing the gauge observation with the estimate from the combination approach.

5. Summary and conclusion

Two new methods have been proposed in this paper, namely the nonparametric Z-R relationship and the dynamic combination approach for the radar and spatially interpolated gauge rainfalls. In this section, uncertainties in each of these methods are discussed in more detail.

The advantage of the traditional parametric relationship ($Z = AR^b$) is that only two parameters need to be estimated. In parametric estimation, every data point influences the inference of the parameters A and b. The disadvantage of a parametric approach is however that a single relationship may not account for all the variations in the data if an incorrect function form is used. In the nonparametric approach, the aim is to use the sample of Z and R to specify the underlying relationship. The idea is that the data points closest to the target point will lead to better regression estimates. As with any statistical approach, the sample Z and

R values need to properly represent the true population, which often requires large amounts of data. In radar rainfall, the Z-R pairs give thousands of data points, which is ideal for applying nonparametric approaches. When there is insufficient data, such as in the case of the highest rainfall rates, parametric approaches can extrapolate and may perform better.

The combination method provides better rainfall estimates compared to the radar or gauge estimates. The advantage of the proposed combination is that it can be used with existing rain gauge and radar networks to estimate rainfall at ungauged locations. The improvement due to the combination method depends on uncertainties in the estimation of the covariance matrix.

This study presents a new method for rainfall estimation from radar reflectivity with greater efficiency compared to a traditional parametric Z-R relationship method. The uncertainty of the parametric Z-R relationship parameters introduces biases into the rainfall estimates. Given the large amount of data available from the radar, a nonparametric approach is attractive. The proposed NPR method is shown to produce more reliable rainfall estimates and to reduce errors by approximately 10% compared to a traditional Z-R relationship, with improvements in the rainfall estimates at around 90% of the locations. In addition, the rainfall estimated using NPR has smaller errors than when spatially interpolated from gauges in the areas of low gauge density.

Further improvements are demonstrated when radar and gauge rainfall estimates are combined. The combination method uses dynamic weights based on the errors from each method. The rainfall estimate from the combination method is about 20% more accurate than the traditional parametric Z-R relationship method and has the lowest error over the entire study domain.

We have shown that over densely gauged areas spatial interpolation can provide good rainfall estimates. The benefit of a radar and gauge combination approach is evident in sparsely gauged areas or when storm periods have large spatial heterogeneity. Under these conditions the dynamic combination of radar and gauge data is recommended. Thus the combination method is not only useful in reducing errors in spatial rainfall estimates, but also in diagnosing the strengths and weaknesses of a particular gauge and radar network.

Acknowledgements

The authors gratefully acknowledge Sydney Water and the Australian Bureau of Meteorology for providing radar rain gauge and radar data for this study. Radar data that has been used in this study can be obtained from the Australian Bureau of Meteorology by placing a request using the Climate Data Services web page (http://www.bom.gov.au/climate/data-services/data-requests.shtml). Rain gauge data that has been used in this paper can be obtained by contacting Sydney Water (http://sydneywater.custhelp.com/app/ask). The authors acknowledge the Australian Research Council for partial funding for this work.

References

Bárdossy, A., 2006. Copula-based geostatistical models for groundwater quality parameters. Water Resour. Res. 42.
Bárdossy, A., Li, J., 2008. Geostatistical interpolation using copulas. Water Resour. Res. 44.
Bennett, N.D., Croke, B.F.W., Guariso, G., Guillaume, J.H.A., Hamilton, S.H., Jakeman, A.J., et al., 2013. Characterising performance of environmental models. Environ. Modell. Softw. 40, 1–20.
Berndt, C., Rabiei, E., Haberlandt, U., 2014. Geostatistical merging of rain gauge and radar data for high temporal resolutions and various station density scenarios. J. Hydrol. 508, 88–101.
Berne, A., Ten Heggeler, M., Uijlenhoet, R., Delobbe, L., Dierickx, P., de Wit, M., 2005. A preliminary investigation of radar rainfall estimation in the Ardennes region and a first hydrological application for the Ourthe catchment. Nat. Hazards Earth Syst. Sci. 5, 267–274.
Burlando, P., Montanari, A., Ranzi, R., 1996. Forecasting of storm rainfall by combined use of radar, rain gages and linear models. Atmos. Res. 42, 199–216.
Calheiros, R.V., Zawadzki, I., 1987. Reflectivity-rain rate relationships for radar hydrology in Brazil. J. Clim. Appl. Meteorol. 26, 118–132.
Chang, C.L., Lo, S.L., Yu, S.L., 2005. Applying fuzzy theory and genetic algorithm to interpolate precipitation. J. Hydrol. 314, 92–104.
Chowdhury, S., Sharma, A., 2009. Long-range niño-3.4 predictions using pairwise dynamic combinations of multiple models. J. Clim. 22, 793–805.
Chowdhury, S., Sharma, A., 2010. Global sea surface temperature forecasts using a pairwise dynamic combination approach. J. Clim. 24, 1869–1877.
Chumchean, S., Seed, A., Sharma, A., 2004. Application of scaling in radar reflectivity for correcting range-dependent bias in climatological radar rainfall estimates. J. Atmos. Oceanic Technol. 21, 1545–1556.
Chumchean, S., Seed, A., Sharma, A., 2006b. Correcting of real-time radar rainfall bias using a Kalman filtering approach. J. Hydrol. 317, 123–137.
Chumchean, S., Sharma, A., Seed, A., 2003. Radar rainfall error variance and its impact on radar rainfall calibration. Phys. Chem. Earth 28, 27–39.
Chumchean, S., Sharma, A., Seed, A., 2006a. An integrated approach to error correction for real-time radar-rainfall estimation. J. Atmos. Oceanic Technol. 23, 67–79.
Ciach, G.J., Morrissey, M.L., Krajewski, W.F., 2000. Conditional bias in radar rainfall estimation. J. Appl. Meteorol. 39, 1941–1946.
Cressie, N., 1988. Spatial prediction and ordinary kriging. Math. Geol. 20, 405–421.
Creutin, J.D., Delrieu, G., Lebel, T., 1988. Rain measurement by raingage-radar combination: a geostatistical approach. J. Atmos. Oceanic Technol. 5, 102–115.
Delrieu, G., Wijbrans, A., Boudevillain, B., Faure, D., Bonnifait, L., Kirstetter, P., 2014. Geostatistical radar–raingauge merging: a novel method for the quantification of rain estimation accuracy. Adv. Water Resour. 71, 110–124.
Devineni, N., Sankarasubramanian, A., 2010. Improved categorical winter precipitation forecasts through multimodel combinations of coupled GCMs. Geophys. Res. Lett. 37, L24704.
García-Pintado, J., Barberá, G.G., Erena, M., Castillo, V.M., 2009. Rainfall estimation by rain gauge-radar combination: a concurrent multiplicative-additive approach. Water Resour. Res. 45, W01415.
Goovaerts, P., 2000. Geostatistical approaches for incorporating elevation into the spatial interpolation of rainfall. J. Hydrol. 228, 113–129.
Goudenhoofdt, E., Delobbe, L., 2009. Evaluation of radar-gauge merging methods for quantitative precipitation estimates. Hydrol. Earth Syst. Sci. 13, 195–203.
Haberlandt, U., 2007. Geostatistical interpolation of hourly precipitation from rain gauges and radar for a large-scale extreme rainfall event. J. Hydrol. 332, 144–157.
Habib, E., Aduvala, A.V., Meselhe, E.A., 2008. Analysis of radar-rainfall error characteristics and implications for streamflow simulation uncertainty. Hydrol. Sci. J. 53, 568–587.
Habib, E., Krajewski, W., Kruger, A., 2001. Sampling errors of tipping-bucket rain gauge measurements. J. Hydrol. Eng. 6, 159–166.
Hasan, M.M., Sharma, A., Johnson, F., Mariethoz, G., Seed, A., 2014. Correcting bias in radar Z–R relationships due to uncertainty in point rain gauge networks. J. Hydrol. 519 (Part B), 1668–1676.
Hazenberg, P., Yu, N., Boudevillain, B., Delrieu, G., Uijlenhoet, R., 2011. Scaling of raindrop size distributions and classification of radar reflectivity–rain rate relations in intense Mediterranean precipitation. J. Hydrol. 402, 179–192.
Henschke, A., Habib, E., Pathak, C., 2009. Adjustment of the Z-R relationship in real-time for use in South Florida. In: World Environmental and Water Resources Congress 2009. American Society of Civil Engineers, pp. 1–12.
Huang, Y., Wong, P., Gedeon, T., 1998. Spatial interpolation using fuzzy reasoning and genetic algorithms. J. Geogr. Inf. Decis. Anal. 2, 204–214.
Hutchinson, M.F., 1998. Interpolation of rainfall data with thin plate smoothing splines. Part II: analysis of topographic dependence. J. Geogr. Inf. Decis. Anal. 2, 152–167.
Hwang, Y., Clark, M., Rajagopalan, B., Leavesley, G., 2012. Spatial interpolation schemes of daily precipitation for hydrologic modeling. Stochastic Environ. Res. Risk Assess. 26, 295–320.
Isaaks, E.H., Srivastava, R.M., 1990. An Introduction to Applied Geostatistics. Oxford University Press, USA.
Jewell, S.A., Gaussiat, N., 2015. An assessment of kriging-based rain-gauge–radar merging techniques. Q. J. R. Meteorol. Soc. 141, 2300–2313.
Kalinga, O.A., Gan, T.Y., 2012. Merging WSR-88D stage III radar rainfall data with rain gauge measurements using wavelet analysis. Int. J. Remote Sens. 33, 1078–1105.
Kazianka, H., 2013. Approximate copula-based estimation and prediction of discrete spatial data. Stochastic Environ. Res. Risk Assess. 27, 2015–2026.
Kazianka, H., 2013. spatialCopula: a Matlab toolbox for copula-based spatial analysis. Stochastic Environ. Res. Risk Assess. 27, 121–135.
Khan, M.Z.K., Mehrotra, R., Sharma, A., Sankarasubramanian, A., 2014. Global sea surface temperature forecasts using an improved multimodel approach. J. Clim. 27, 3505–3515.
Kitzmiller, D., Miller, D., Fulton, R., Ding, F., 2013. Radar and multisensor precipitation estimation techniques in national weather service hydrologic operations. J. Hydrol. Eng. 18, 133–142.
Krajewski, W.F., 1987. Cokriging radar-rainfall and rain gage data. J. Geophys. Res. 92, 9571–9580.
Krajewski, W.F., Smith, J.A., 2002. Radar hydrology: rainfall estimation. Adv. Water Resour. 25, 1387–1394.
Kurtzman, D., Navon, S., Morin, E., 2009. Improving interpolation of daily precipitation for hydrologic modelling: spatial patterns of preferred interpolators. Hydrol. Processes 23, 3281–3291.

Lall, U., Sharma, A., 1996. A nearest neighbor bootstrap for resampling hydrologic time series. Water Resour. Res. 32, 679–693.
Lee, G.W., Zawadzki, I., 2005. Variability of drop size distributions: time-scale dependence of the variability and its effects on rain estimation. J. Appl. Meteorol. 44, 241–255.
Li, J., Bárdossy, A., Guenni, L., Liu, M., 2011. A copula based observation network design approach. Environ. Modell. Softw. 26, 1349–1357.
Mapiam, P.P., Sriwongsitanon, N., Chumchean, S., Sharma, A., 2009. Effects of rain gauge temporal resolution on the specification of a Z-R relationship. J. Atmos. Oceanic Technol. 26, 1302–1314.
Marshall, J.S., Palmer, W.M., 1948. The distribution of raindrops with size. J. Appl. Meteorol. 5.
Martens, B., Cabus, P., De Jongh, I., Verhoest, N.E.C., 2013. Merging weather radar observations with ground-based measurements of rainfall using an adaptive multiquadric surface fitting algorithm. J. Hydrol. 500, 84–96.
Méndez-Antonio, B., Magaña, V., Caetano, E., Da silveira, R.B., Domínguez, R., 2009. Analysis of daily precipitation based on weather radar information in México City. Atmósfera 22, 299–313.
Ochou, A., Zahiri, E., Bamba, B., Koffi, M., 2011. Understanding the variability of Z-R relationships caused by natural variations in raindrop size distributions (DSD): implication of drop size and number. Atmos. Clim. Sci. 1, 147–164.
Okabe, A., Boots, B., Sugihara, K., Chiu, S.N., 2009. Spatial Tessellations: Concepts and Applications of Voronoi Diagrams. John Wiley & Sons.
Oriani, F., Straubhaar, J., Renard, P., Mariethoz, G., 2014. Simulation of rainfall time series from different climatic regions using the direct sampling technique. Hydrol. Earth Syst. Sci. 18, 3015–3031.
Piman, T., Babel, M.S., Das Gupta, A., Weesakul, S., 2007. Development of a window correlation matching method for improved radar rainfall estimation. Hydrol. Earth Syst. Sci. 11, 1361–1372.
Prat, O.P., Barros, A.P., 2009. Exploring the transient behavior of Z–R relationships: implications for radar rainfall estimation. J. Appl. Meteorol. Climatol. 48, 2127–2143.
Rabiei, E., Haberlandt, U., 2015. Applying bias correction for merging rain gauge and radar data. J. Hydrol. 522, 544–557.
Rosenfeld, D., Amitai, E., 1998. Comparison of WPMM versus regression for evaluating Z–R relationships. J. Appl. Meteorol. 37, 1241–1249.
Rosenfeld, D., Wolff, D.B., Amitai, E., 1994. The window probability matching method for rainfall measurements with radar. J. Appl. Meteorol. 33, 682–693.
Rosenfeld, D., Wolff, D.B., Atlas, D., 1993. General probability-matched relations between radar reflectivity and rain rate. J. Appl. Meteorol. 32, 50–72.
Schiemann, R., Erdin, R., Willi, M., Frei, C., Berenguer, M., Sempere-Torres, D., 2011. Geostatistical radar-raingauge combination with nonparametric correlograms: methodological considerations and application in Switzerland. Hydrol. Earth Syst. Sci. 15, 1515–1536.
Seed, A., Nicol, J., Austin, G.L., Stow, C.D., Bradley, S.G., 1996. The impact of radar and raingauge sampling errors when calibrating a weather radar. Meteorol. Appl. 3, 43–52.
Seed, A.W., Jordan, P.W., 2002. Mapview Radar Rainfall Visualisation and Processing Software, Version 2.6. The Australian Bereau of Meteorology.
Seo, D.-J., 1998. Real-time estimation of rainfall fields using radar rainfall and rain gage data. J. Hydrol. 208, 37–52.
Seo, D.-J., 2013. Conditional bias-penalized kriging (CBPK). Stochastic Environ. Res. Risk Assess. 27, 43–58.
Seo, D.-J., Breidenbach, J.P., 2002. Real-time correction of spatially nonuniform bias in radar rainfall data using rain gauge measurements. J. Hydrometeorol. 3, 93–111.
Seo, D.-J., Seed, A., Delrieu, G., 2013. Radar and multisensor rainfall estimation for hydrologic applications. In: Rainfall: State of the Science. American Geophysical Union, pp. 79–104.
Seo, D.-J., Siddique, R., Zhang, Y., Kim, D., 2014. Improving real-time estimation of heavy-to-extreme precipitation using rain gauge data via conditional bias-penalized optimal estimation. J. Hydrol. 519 (Part B), 1824–1835.
Severino, E., Alpuim, T., 2005. Spatiotemporal models in the estimation of area precipitation. Environmetrics 16, 773–802.
Sharma, A., Lall, U., Tarboton, D.G., 1998. Kernel bandwidth selection for a first order nonparametric streamflow simulation model. Stochastic Hydrol. Hydraul. 12, 33–52.
Sharma, A., Mehrotra, R., 2014. An information theoretic alternative to model a natural system using observational information alone. Water Resour. Res. 50, 650–660.
Sharma, A., O'Neill, R., 2002. A nonparametric approach for representing interannual dependence in monthly streamflow sequences. Water Resour. Res. 38 5-1-5-10.
Sharma, A., Tarboton, D.G., Lall, U., 1997. Streamflow simulation: a nonparametric approach. Water Resour. Res. 33, 291–308.
Shucksmith, P.E., Sutherland-Stacey, L., Austin, G.L., 2011. The spatial and temporal sampling errors inherent in low resolution radar estimates of rainfall. Meteorol. Appl. 18, 354–360.
Sideris, I.V., Gabella, M., Erdin, R., Germann, U., 2014. Real-time radar-rain-gauge merging using spatio-temporal co-kriging with external drift in the alpine terrain of Switzerland. Q. J. R. Meteorol. Soc. 140, 1097–1111.
Silverman, B.W., 1986. Density Estimation for Statistics and Data Analysis. CRC press.
Sinclair, S., Pegram, G., 2005. Combining radar and rain gauge rainfall estimates using conditional merging. Atmos. Sci. Lett. 6, 19–22.
Smith, J.A., Krajewski, W.F., 1991. Estimation of the mean field bias of radar rainfall estimates. J. Appl. Meteorol. 30, 397–412.
Steiner, M., Smith, J.A., Burges, S.J., Alonso, C.V., Darden, R.W., 1999. Effect of bias adjustment and rain gauge data quality control on radar rainfall estimation. Water Resour. Res. 35, 2487–2503.
Steiner, M., Smith, J.A., Uijlenhoet, R., 2004. A microphysical interpretation of radar reflectivity–rain rate relationships. J. Atmos. Sci. 61, 1114–1131.
Timmermann, A., 2006. Chapter 4 forecast combinations. In: Elliott, C.W.J.G.G., Timmermann, A. (Eds.), Handbook of Economic Forecasting. Elsevier, pp. 135–196.
Uijlenhoet, R., 2001. Raindrop size distributions and radar reflectivity? Rain rate relationships for radar hydrology. Hydrol. Earth Syst. Sci. Discussions 5, 615–628.
Velasco-Forero, C.A., Sempere-Torres, D., Cassiraga, E.F., Jaime Gómez-Hernández, J., 2009. A non-parametric automatic blending methodology to estimate rainfall fields from rain gauge and radar data. Adv. Water Resour. 32, 986–1002.
Verrier, S., Barthès, L., Mallet, C., 2013. Theoretical and empirical scale dependency of Z-R relationships: evidence, impacts, and correction. J. Geophys. Res. 118, 7435–7449.
Villarini, G., Krajewski, W.F., 2010. Review of the different sources of uncertainty in single polarization radar-based estimates of rainfall. Surv. Geophys. 31, 107–129.
Villarini, G., Serinaldi, F., Krajewski, W.F., 2008. Modeling radar-rainfall estimation uncertainties using parametric and non-parametric approaches. Adv. Water Resour. 31, 1674–1686.
Wang, G., Liu, L., Ding, Y., 2012. Improvement of radar quantitative precipitation estimation based on real-time adjustments to Z-R relationships and inverse distance weighting correction schemes. Adv. Atmos. Sci. 29, 575–584.
Wasko, C., Sharma, A., Rasmussen, P., 2013. Improved spatial prediction: a combinatorial approach. Water Resour. Res. 49, 3927–3935.